Evaluation of Induced Radioactivity Generated during LHD Deuterium Plasma Experiments*)

Sachiko YOSHIHASHI, Hayato YAMADA, Makoto KOBAYASHI[1)], Takeo NISHITANI, Atsushi YAMAZAKI, Mitsutaka ISOBE[1)], Kunihiro OGAWA[1)] and Akira URITANI

Nagoya University, Furo-cho, Chikusa-ku, Nagoya 464-8603, Japan
[1)]*National Institute for Fusion Science, 322-6 Oroshi-cho, Toki 509-5292, Japan*

(Received 7 January 2022 / Accepted 30 June 2022)

Neutrons are generated in a fusion plasma and induce various radionuclides via a nuclear reaction with fusion reactor materials. Evaluating the kinds of nuclide and the amount of induced radioactivity is important for decommissioning planning and regular maintenance. In this study, we verified a long-term prediction model of induced radioactivity in the large helical device (LHD) model by comparing induced radioactivity generated during deuterium plasma experiments in LHD with results calculated using a high-energy particle-induced radioactivity code. The metals employed for activation were SUS316L, Co, Mo, and Ni. During the deuterium plasma experiments, these materials were placed on an 8-O port of the LHD, and the induced radioactivity was measured weekly. To computed induced radioactivity using DCHAIN-SP, the neutron energy spectrum was computed using the LHD model with the Monte-Carlo simulation code PHITS. Although the calculated and measured radioactivity of ^{58}Co and ^{54}Mo agreed well, the calculated values of ^{60}Co and ^{99}Mo were underestimated. However, low-energy components could be improved by incorporating peripheral devices into the LHD model, resulting in more accurate radioactivity predictions.

Keywords: neutron, induced radioactivity, activation, LHD, decommissioning

DOI: 10.1585/pfr.17.2405096

1. Introduction

Fast neutrons with 2.45 MeV energy are generated in deuterium plasma experiments performed in the Large Helical Device (LHD) by the d(d,n)^{3}He reaction. Neutrons generated during the deuterium plasma experiments activate the LHD and peripheral equipment, resulting in low-level radioactivity. The assessment of the kind of nuclide and the amount of induced radioactivity is important for the LHD decommissioning planning and regular maintenance.

To understand the behavior of neutrons in deuterium plasma experiments, we created a LHD model using the neutron transport Monte-Carlo simulation code PHITS [1–3]. In a previous study, a neutron spectrum in a vacuum vessel of the LHD was obtained via activation experiments using multiple activation foils [4]. The reaction rate of each activation foil was generally consistent with the LHD model calculation [5,6]. Additionally, the spatial distributions of thermal and epithermal neutrons in the LHD torus hall were investigated using the LHD model.

In this study, we develop a prediction code for the amount of activation in a vacuum vessel of the LHD and peripheral equipment using the LHD model. However, experimental data on the amount of activation produced by the deuterium plasma experiment are insufficient. Therefore, we performed an activation experiment of LHD structural materials during the deuterium plasma experiments and compared it with the calculation results of the LHD model to verify the effectiveness of the LHD model.

2. Experiments

The activation experiment was performed in the 22nd campaign of the LHD experiment. For the activation experiment, four metal materials—Cobalt (Co), Nickel (Ni), Molybdenum (Mo), and SUS316L(SUS)—were prepare. SUS was used mainly in the LHD body and peripherals. We chose the ^{54}Fe(n,p)^{54}Mn reaction since Fe is the most abundant element in SUS.

Three pure metals contributed significantly to the activation of SUS316L and were used for evaluating the amount of activation, excluding the influence of other materials. Table 1 shows the reaction, produced nuclides, thresholds, and half-lives of each material [7]. Figure 1 shows the reaction cross-sections of ^{59}Co and ^{98}Mo.

These materials were placed on an 8-O port of LHD during the deuterium plasma experiments. The materials were removed once a week, and the gamma-rays shown in Table 1 were measured using high-purity germanium (HPGe) semiconductor detector (GX3018-7935 -7 RDC-4-2002C, Canberra). After measurement, the materials

author's e-mail: s-yoshihashi@energy.nagoya-u.ac.jp
*) This article is based on the presentation at the 30th International Toki Conference on Plasma and Fusion Research (ITC30).

Table 1 Metal materials used in the experiment and each radionuclide [7].

Material	Reaction	Size (mm)	Threshold	Half-life	Gamma energy
Co	^{59}Co (n, γ) ^{60}Co	16.7×16.7×0.4		5.27 year	1173 keV, 1333 keV
Mo	^{98}Mo (n, γ) ^{99}Mo	33.3×33.3×0.1		65.9 hour	141 keV, 181 keV, 740 keV
Ni	^{58}Ni (n, p) ^{58}Co	20×20×0.8	0.5 MeV	70.9 day	811 keV
SUS316L	^{54}Fe (n, p) ^{54}Mn	50×50×0.3	1.0 MeV	312 day	835 keV

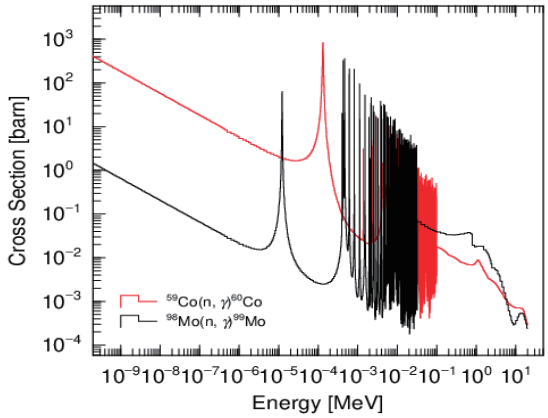

Fig. 1 The cross-sections of ^{59}Co(n,γ)^{60}Co and ^{98}Mo(n,γ)^{99}Mo [8–10].

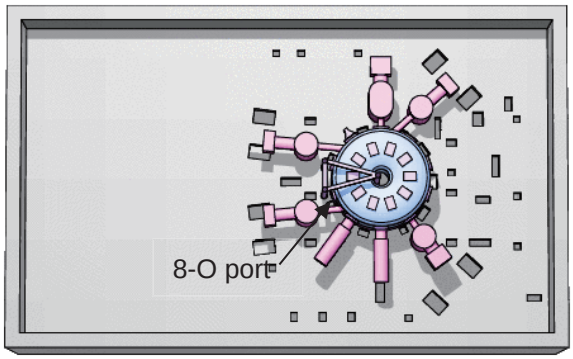

Fig. 2 The three-dimensional LHD model for the neutron calculation.

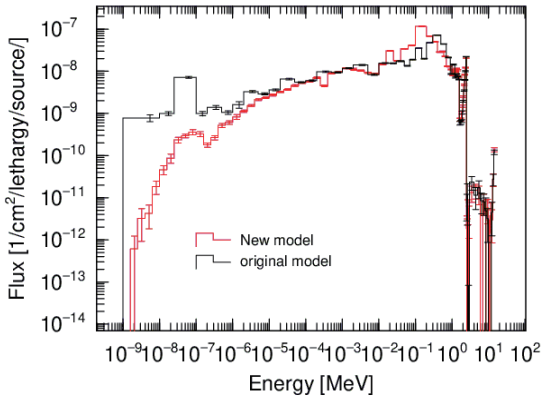

Fig. 3 The neutron energy spectrum on the 8-O port.

were placed again in the same position on the 8-O port. During the 22nd campaign, the materials were measured a total of eight times.

When the peak count rate measurement in the HPGe detector is n, the source's radioactivity A can be calculated as follows:

$$A = n/I_\gamma\varepsilon, \quad (1)$$

where I_γ is the gamma-ray emission probability per decay of the source nuclide and ε is the peak detection efficiency of the peak detector. Additionally, the measurement time was 300 s, which was sufficiently shorter than the half-life of these nuclides; thus, the decay of radioactivity during the measurement is not considered.

3. Calculation

The neutron energy spectrum of the 8-O port was calculated using a Monte-Carlo simulation code PHITS ver. 3.26 [8] with the JENDL-4.0 nuclear data [9–11]. The activation calculations were performed using a high-energy particle-induced radioactivity calculation code DCHAIN-SP [12].

Figure 2 shows the three-dimensional LHD model created by PHITS. Although the LHD model reproduces the LHD main unit, including NB injectors and a vacuum pumping port, the walls, floor, and ceiling of the LHD torus hall and other peripherals are exclude. The inner construction of the LHD vacuum vessel is the same as in ref (2). A disk-shaped cell was installed in the 8-O port of the LHD model, and the neutron energy spectrum inside the cell was obtained. The arrows in Fig. 2 indicate the 8-O port. Figure 3 shows the energy spectrum of the 8-O port calculated using the LHD model. The black lines show the energy spectra obtained in ref. 4 (original model). Also, a neutron energy spectrum in a wide energy range, which is evaluated by an unfolding technique using the SAND-II code [13] with the measurements by multiple activation foils, is shown in ref. 4. The experimentally evaluated spectrum roughly matched the calculated spectrum; the calculated spectrum was smaller than the experimentally evaluated spectra at energies of 10^{-2} MeV or lower.

The neuron capture of ^{59}Co and ^{98}Mo used in the experiment occur in the low-energy region, as shown in Fig. 1. To obtain an accurate energy spectrum, the flange of the 8-O port was precisely modeled (detailed model) and

calculated by narrowing the energy bin in the low-energy region. Figure 4 shows the flange structure of the 8-O port of the original and detailed models. The red line in Fig. 3 represents the energy spectrum obtained from the detailed model. The use of the detailed model significantly reduced the flux in the thermal neutron region. On the other hand, the flux above 10 eV - 5 MeV increased.

The calculation method for the amount of activation using DCHAIN-SP is as follows. First, the PHITS-modeled irradiation material is irradiated with neutrons in the energy spectrum of the 8-O port to generate an input file for DCHAIN-SP. After that, the induced radioactivity at the measurement time was calculated by DCHAIN-SP using the input file. The input file requires the neutron irradiation time and cooling time. In the deuterium plasma experiment, the LHD plasma is repeatedly turned on and off and neutrons are generated only for a few seconds each time the LHD is turned on. However, the half-lives of ^{60}Co, ^{58}Co and ^{54}Mn are sufficiently lengthy and independent of this detailed cycle. Therefore, in these induced radioactivity calculations, the experimental time per day is first set from 10:00 to 20:00, and the sample is irradiated with the cumulated neutron yield per day. After that, the cooling time is set from 20:00 to 10:00 the next day. This irradiation cycle is repeated for one week, and the calculated induced radioactivity is compared with the experimental results. On the other hand, since ^{99}Mo has a short half-life, the induced radioactivity is calculated every hour using the cumulative neutron yield for the hour.

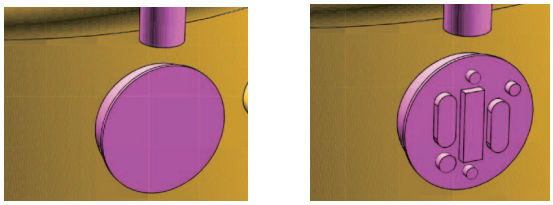

(a) Original model (b) Detailed model

Fig. 4 The flange structure of the 8-O port.

4. Results and Discussions

4.1 Induced radioactivity

Figure 5 shows the residual radioactivity of each nuclide measured weekly by the HPGe detector. The black circles and bars represent the induced radioactivity and cumulative neutron yield, respectively. The neutron yield indicates the total number of neutrons generated in the LHD.

Because ^{60}Co has a sufficiently long half-life, its residual radioactivity does not decrease during the experiment; rather, it increases as the total neutron yield increases. The residual radioactivity of ^{99}Mo with a short half-life fluctuated following the influence of the neutron yield each week. Since the half-life of ^{58}Co and ^{54}Mn is less than one year, each of their residual radioactivity is gradually

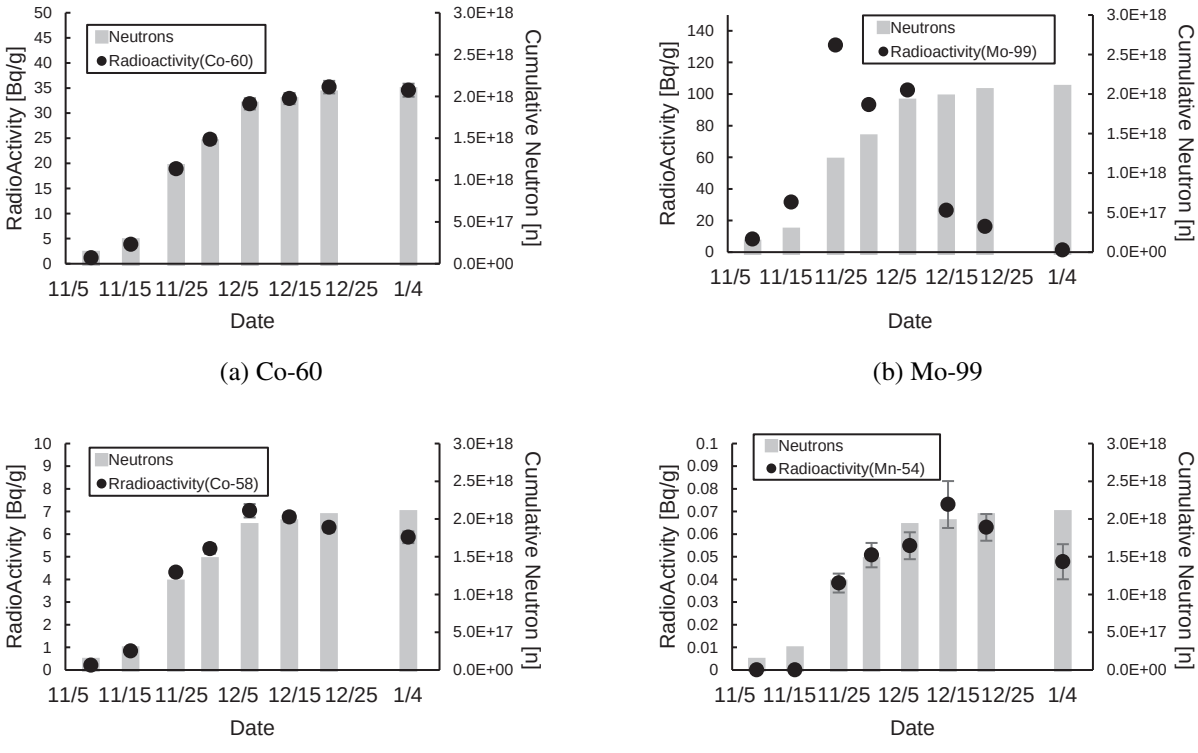

(a) Co-60 (b) Mo-99

(c) Co-58 (d) Mn-54

Fig. 5 Weekly induced radioactivity of each nuclide.

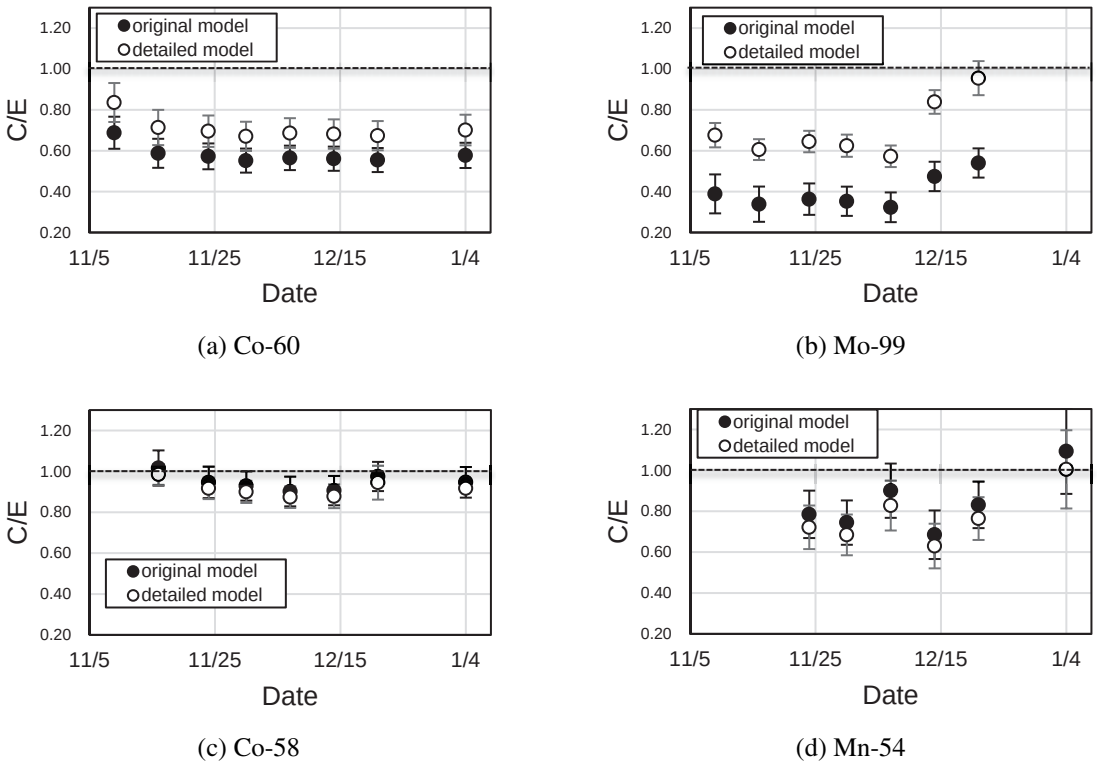

(a) Co-60

(b) Mo-99

(c) Co-58

(d) Mn-54

Fig. 6 Ratio of the calculated value to the experimental value (C/E).

decaying.

The measurement results showed the relationship between the half-life and the neutron yield.

4.2 Comparison of measurement and calculation values

Figure 6 shows the ratio of the calculated to experimental value (C/E) or each nuclide. The black and white circles represent the results calculated using energy spectra obtained from the original and detailed models, respectively (Fig. 3). The error bars represent the statistical error in the calculations.

When using the results of the energy spectrum from the original model the radioactivity of ^{60}Co and ^{99}Mo in Figs. 6 (a) and 6 (b) are significantly smaller than the experimental value. The C/E of ^{60}Co and ^{99}Mo are 0.6 and 0.4, respectively. These nuclides are produced via a neutron capture reaction that has a greater reaction cross-section at low energy. The flux from 10^{-5} to 10^{-1} MeV was increased by modeling the 8-O port in detail; therefore, the calculated values are close to the experimental values. Although the energy spectrum is improved by modeling the flange of the 8-O port, the calculated values are still smaller than the experimental values, possibly because the equipment around the LHD was not incorporated into the detailed model. Further improvement of the energy spectrum can be expected by incorporating the equipment structures into the model, and the precision of the induced radioactivity calculations will be improved.

Figures 6 (c) and 6 (d) show the C/E of ^{58}Co and ^{54}Mn respectively. The C/E of ^{58}Co calculated using the energy spectrum of the original model is approximately 0.9, indicating that the calculated and experimental values are in good agreement. Furthermore, the results obtained using the original and detailed models were almost the same. Consequently, we confirmed that the energy spectrum of the detailed model accurately reproduces the neutron energy on the 8-O port.

The nuclide ^{54}Mn is produced via an n-p reaction with fast neutrons, as with the nuclide ^{58}Co. However, the C/E of ^{54}Mn was lower than that of ^{58}Co. A reason for the discrepancy in C/E would be that the small radioactivity of ^{54}Mn in the activation experiment due to a small cross-section led to uncertainty in the radioactivity measurement.

5. Conclusion

To evaluate the amount of activation of the LHD and peripheral equipment in deuterium plasma experiments via numerical simulation, induced radioactivity generated during the experiments was compared with the induced radioactivity calculated using PHITS and DCHAIN-SP.

The calculated values of radioactivity approached the measured value after recalculating the neutron energy spectrum at a metal sample installation position by reviewing the LHD model.

The reliability of the LHD model is proven by the calculation of the amount of activation and by comparison of experiments.

In the future, we will calculate the amount of ac-

tivation for other materials. Additionally, we will estimate medium and long-term induced radioactivity using DCHAIN-SP.

[1] T. Nishitani *et al.*, Plasma Fusion Res. **11**, 2405057 (2016).
[2] T. Nishitani *et al.*, Fusion Eng. Des. **123**, 1020 (2017).
[3] Y. Nakano *et al.*, Plasma Fusion Res. **9**, 3405141 (2014).
[4] T. Tanaka *et al.*, Fusion Eng. Des. **146**, 496 (2019).
[5] T. Tanaka *et al.*, Plasma Fusion Res. **14**, 3405162 (2019).
[6] M. Kobayashi *et al.*, Plasma Fusion Res. **15**, 2405043 (2020).
[7] R.B. Firestone, Table of Isotopes, 8th edition (John Wiley & Sons, Inc., 1996).
[8] T. Sato *et al.*, J. Nucl. Sci. Technol. **55**, 684 (2018).
[9] K. Shibata *et al.*, J. Nucl. Sci. Technol. **48**(1), 1 (2011).
[10] O. Iwamoto *et al.*, J. Korean Phys. Soc. **59**(2), 1224 (2011).
[11] G. Chiba *et al.*, J. Nucl. Sci. Technol. **48**(2), 172 (2011).
[12] T. Kai *et al.*, JAERI-Data/Code 2001-016. **3** (2001).
[13] P.J. Griffin *et al.*, User's Manual for SNL-SAND-II Code, Sandia National Labs (1994).